The Effect of Tin on the Formation and Properties of Pt/MgAl(Sn)Ox Catalysts for Dehydrogenation of Alkanes

Belskaya, O. B.; Stepanova, L. N.; Nizovskii, A. I.; Kalinkin, A. V.; Erenburg, S. B.; Trubina, S. V.; Kvashnina, K. O.; Leont'Eva, N. N.; Gulyaeva, T. I.; Trenikhin, M. V.; Bukhtiyarov, V. I.; Likholobov, V. A.;

Originally published:

December 2018

Catalysis Today 329(2019), 187-196

DOI: https://doi.org/10.1016/j.cattod.2018.11.081

Title: The Effect of Tin on the Formation and Properties of Pt/MgAl(Sn)O_x Catalysts for Dehydrogenation of Alkanes

Authors: O.B. Belskaya, L.N. Stepanova, A.I. Nizovskii, A.V. Kalinkin, S.B. Erenburg, S.V. Trubina, K.O. Kvashnina, N.N. Leont'eva, T.I. Gulyaeva, M.V. Trenikhin, V.I. Bukhtiyarov, V.A. Likholobov

PII: S0920-5861(18)31350-6
DOI: https://doi.org/10.1016/j.cattod.2018.11.081
Reference: CATTOD 11817

To appear in: *Catalysis Today*

Received date: 3 August 2018
Revised date: 13 November 2018
Accepted date: 30 November 2018

Please cite this article as: Belskaya OB, Stepanova LN, Nizovskii AI, Kalinkin AV, Erenburg SB, Trubina SV, Kvashnina KO, Leont'eva NN, Gulyaeva TI, Trenikhin MV, Bukhtiyarov VI, Likholobov VA, The Effect of Tin on the Formation and Properties of Pt/MgAl(Sn)O_x Catalysts for Dehydrogenation of Alkanes, *Catalysis Today* (2018), https://doi.org/10.1016/j.cattod.2018.11.081

The Effect of Tin on the Formation and Properties of Pt/MgAl(Sn)O_x Catalysts for Dehydrogenation of Alkanes

O.B. Belskaya[a,b*], L.N. Stepanova[a], A.I. Nizovskii[b,c], A.V. Kalinkin[c], S.B. Erenburg[d,e], S.V. Trubina[e], K.O. Kvashnina[f,g], N.N. Leont'eva[a], T.I. Gulyaeva[a] M.V. Trenikhin[a,b], V.I. Bukhtiyarov[c], V.A. Likholobov[a]

[a] *Institute of Hydrocarbons Processing SB RAS, Neftezavodskaya Str., 54, 644040 Omsk, Russia*

[b] *Omsk State Technical University, Mira Ave., 11, 644050 Omsk, Russia*

[c] *Boreskov Institute of Catalysis SB RAS, Acad. Lavrentieva Ave., 5, 630090 Novosibirsk, Russia*

[d] *Nikolaev Institute of Inorganic Chemistry SB RAS, Acad. Lavrentieva Ave., 3, 630090 Novosibirsk, Russia*

[e] *Budker Institute of Nuclear Physics SB RAS, Acad. Lavrentieva Ave., 11, 630090 Novosibirsk, Russia*

[f] *ESRF, 38043, Grenoble, France*

[g] *HZDR, Institute of Resource Ecology, 01314, Dresden, Germany*

Corresponding author: Olga B. Belskaya
Present address: Institute of Hydrocarbons Processing, Siberian Branch of the Russian Academy of Sciences, Neftezavodskaya Str., 54, 644040 Omsk, Russia
E-mail: obelska@ihcp.ru
Tel.: +7 (3812) 670 474, fax: +7 (3812) 646 156

Graphical abstract

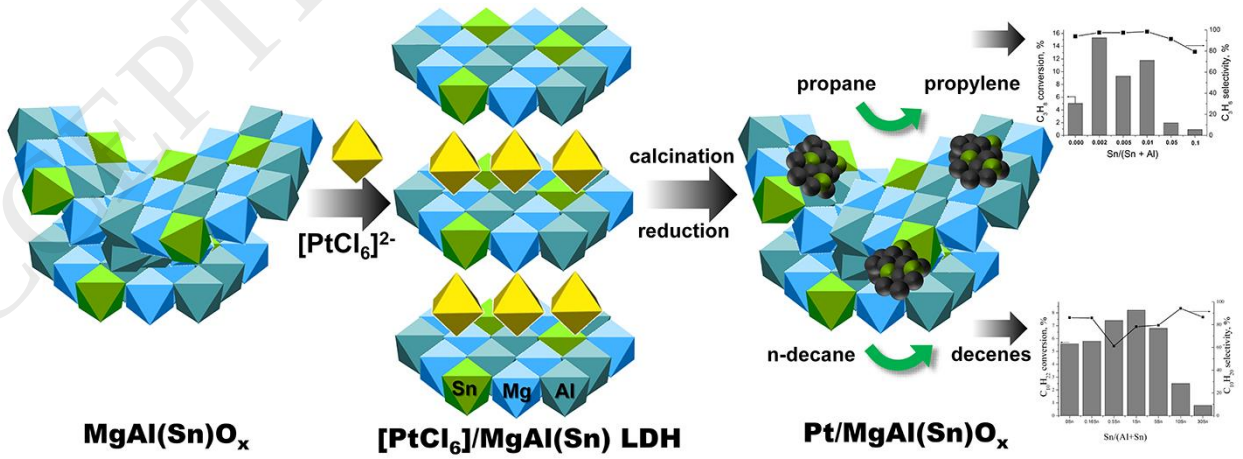

Highlights

- Tin containing layered double hydroxides (LDH) synthesis.

- Propane and n-decane dehydrogenation on the platinum catalysts based on $MgAl(Sn)O_x$.
- Electronic state of platinum in the $Pt/MgAl(Sn)O_x$ catalysts.

ABSTRACT

The MgAl(Sn) layered double hydroxides (LDH) with the atomic ratios Mg/(Al+Sn) = 3 and Sn/(Sn+Al) = 0, 0.002, 0.005, 0.01, 0.05, 0.1, 0.3, 0.5, 0.7, 1.0 were synthesized and the ratio Sn/(Sn+Al) $\leq$ 0.1 was shown to provide the formation of systems with uniform phase composition. Mixed oxides derived from LDH retain the high specific surface area of 150-200 m^2/g and the basic properties when some aluminium atoms are replaced with tin. It was found that the Sn-containing mixed oxides are able to restore the layered structure during rehydration and intercalate the anion precursors of platinum into the interlayer space of the formed LDH. The emerging platinum sites initiate the reduction of tin at temperatures below 723 K. TEM, EXAFS and XPS studies demonstrated that tin introduction in the support increases the dispersion of supported platinum. An extreme dependence of the activity of $Pt/MgAl(Sn)O_x$ catalysts in propane and n-decane dehydrogenation on the tin content in the support was revealed. The active catalysts are characterized by the phase and elemental uniformity of the support, highly disperse state of Pt(0), and the absence of a noticeable amount of reduced tin and bimetallic particles.

Keywords: tin containing layered double hydroxides, platinum catalysts, propane dehydrogenation, n-decane dehydrogenation, XPS, EXAFS

1. Introduction

Tin is one of the most used platinum modifiers in the catalysts for industrially important processes, such as gasoline reforming, CO oxidation, and selective hydrogenation of the carbonyl group in unsaturated aldehydes [1-3]. The platinum-tin composition is also used in the catalysts for dehydrogenation of alkanes [4-7]. This reaction is highly relevant today due to the possibility of selective production of high-purity alkenes that are necessary for organic synthesis and petrochemistry. The influence of tin on the catalytic properties of platinum catalysts is related to both the structural ("ensemble") and electron effects [8-14]. The precise composition and structure of the PtSn catalytic sites remain debatable; nevertheless, it is believed that the role of tin in the composition of platinum-tin catalysts is closely associated with the degree of its oxidation. It is supposed that tin and platinum form bimetallic alloys of various compositions that provide the dissociative adsorption of alkanes and weaken the adsorption of the target products – alkenes. At the same time, it is established that Sn^0 can serve as a catalytic poison, whereas Sn^{4+} or Sn^{2+} can act as promoters [13, 14]. It is worth noting that the state of tin depends on the content of supported metals, Sn/Pt ratio, nature of the support, pretreatment conditions, and method of the catalyst synthesis [8, 10, 11, 15-18].

The main method used to synthesize bimetallic platinum-tin catalysts is the consecutive or simultaneous impregnation of the support with solutions of metal precursors conventionally represented by hydrochloric acid solutions of $H_2[PtCl_6]$ and $SnCl_2$ [8-22]. These methods do not

provide a significant interaction between tin and platinum, and features of the solvent and the order in which the components are introduced can strongly affect the properties of the obtained catalysts. Anchoring of the previously synthesized PtSn complexes can strengthen the interaction of the metals. When bimetallic complexes are employed, both metals are deposited on the support surface as a single compound, thus making more probable the formation of an alloy after thermal treatment [20-23]. Such complexes are low stable in a water medium, so they are usually anchored in the presence of organic solvents. The approaches based on the chemistry of organometallic compounds, which allow a selective anchoring of tin on the surface of platinum particles, are also efficient for the preparation of PtSn catalysts because they provide an accurate control of atomic arrangement. However, the preparation of bimetallic systems by this method is a complex multistep procedure, especially for practical application [24-26].

Features of the support also exert a significant effect on the properties of Pt-Sn catalysts [27, 28]. Many processes involve γ-Al_2O_3 as the catalyst support, including the commercial dehydrogenation of light alkanes, Oleflex (UOP) [4]. The typical Oleflex catalyst contains a platinum-tin composition. In addition, a basic promoter is introduced into the catalyst to inhibit coke formation initiated by the acid sites of the support. Among non-acid supports, most promising for dehydrogenation of alkanes are those containing aluminum-magnesium oxides, which are synthesized from the corresponding layered double hydroxides. Such oxide supports have moderate and controllable basicity, high thermal stability, and developed surface area [29-31]. Layered double hydroxides (LDH) or hydrotalcite-like materials have the general formula and consist of brucite-like layers where bivalent M^{2+} cations are partially isomorphously substituted by trivalent M^{3+} cations with nearly equal ionic radii (in the case of MgAl-LDH, magnesium cations are substituted by aluminium cations). Therewith, the excessive positive charge of the layers is compensated by hydrated anions A^{n-} located in the interlayer spaces. After calcination at a temperature above 673-923 K, the layered structure is destroyed with the formation of the mixed oxide phase.

Many works describe the dehydrogenation catalysts of various composition synthesized with this type of supports, particularly those containing the PtSn composition [32-40]. It was shown [32] that PtSn/Mg(Al)O catalysts are more active and stable than conventional PtSn/Al_2O_3 in dehydrogenation of light alkanes. In [33], the catalysts were obtained by impregnation of MgAl-LDH with a solution containing the previously synthesized complex $[PtCl_2(SnCl_3)]^{2-}$. In [34], in the first synthesis step, supported platinum particles were anchored on the surface of calcined MgAl-LDH using the acetylacetonate complex, and then tin was introduced as a solution of tetra-n-butyl tin in decane in an argon medium. In [40], to synthesize PtSn-catalysts, LDH was kept for a long time at 343 K in an aqueous solution containing K_2PtCl_6

and Na_2SnO_3 salts. The authors suggest that these conditions make possible the exchange of interlayer anions CO_3^{2-} of the support with $PtCl_6^{2-}$ and SnO_3^{2-} anions; however, the paper does not present data confirming such changes in the composition of interlayer space of LDH.

As follows from the analysis of literature, Sn is usually introduced into platinum catalysts by impregnating the support with tin compounds. One of efficient methods for introducing the modifier is its incorporation into the structure of the oxide support precursor, LDH. Thus, in some studies [36-39, 41], the properties of platinum were modified by the introduction of indium, gallium and zinc cations into MgAl-LDH during coprecipitation of hydroxides. At the same time, the synthesis of Sn-containing LDH is described only in a few [42-44], and there is no information on the use of such systems for the synthesis of supported catalysts.

Thus, our study was aimed to reveal the modifying effect of tin in the composition of aluminum-magnesium oxide support on the properties of supported platinum. The novelty of the work consists in the introduction of tin as the modifying agent via its incorporation into the structure of the support precursor, LDH. To provide the best interaction of platinum with the modifying cation, platinum was anchored by intercalation of the anionic Pt(IV) chloride complexes into the interlayer space of LDH, as it was made in [41, 45-47]. In addition, this method of synthesis allowed using aqueous solutions of the metal complex. In the study, Sn-containing LDH were synthesized upon variation of the tin content; mixed oxides derived from LDH were characterized. The electronic state and dispersion of supported platinum and the properties of Pt/MgAl(Sn)O_x catalysts in dehydrogenation of propane and n-decane were studied.

2. Experimental

2.1. Catalyst preparation

The synthesis of MgAl- and MgAl(Sn)-layered hydroxides was performed by coprecipitaiton. For this purpose, aqueous solutions of metal chlorides ($MgCl_2$, $AlCl_3$, $SnCl_4$) with the concentrations providing the cationic ratios Mg/(Al+Sn) = 3 and Sn/(Sn+Al) = 0, 0.002, 0.005, 0.01, 0.05, 0.1, 0.3, 0.5, 0.7, 1.0 were added to aqueous solution of sodium carbonate (C = 1 mol/L) with the rate of 60 ml/min under vigorous stirring. The synthesis temperature was kept stable at 333 K with pH 10 (by adding NaOH with the concentration of 1 mol/L). The resulting precipitates of layered hydroxides with the carbonate interlayer anions MgAl(Sn)-CO_3 were aged at the synthesis temperature, washed down to the neutral pH of rinsing water, and dried for 16 h at a temperature of 353 K. For the oxide phase MgAl(Sn)O_x, the obtained LDH were calcined at 823 K.

The sorption of chloroplatinic acid (AURAT Co., specs 6-09-2026-87) was carried out from the excess of aqueous solutions using the $MgAl(Sn)O_x$ support. The weight ratio of the support and solution was 1:25. When the mixed oxide contacted aqueous solution of the active component precursor, it rehydrated with reduction of the layered hydroxide structure ("the memory effect") and simultaneous incorporation of $[PtCl_6]^{2-}$ anions into the interlayer space of LDH [41, 45-47]. The chosen method enabled the complete extraction of the metal complex from the impregnating solution. When using the solutions with the platinum concentrations of 0.6 and 2.1 mol/L, the catalysts with the platinum content of 0.3 and 1.0 wt.% were obtained.

Before studying by physicochemical methods, the hydroxide precursors of supports were calcined at a temperature of 823 K, while LDH with the supported ($MgAl(Sn)$-$PtCl_6$) complexes were calcined and reduced by hydrogen at 823 K. The concentrations of magnesium, tin, aluminum and platinum in the initial solutions and solid samples after their dissolution were determined by inductively coupled plasma atomic emission spectroscopy on a Varian 710-ES device.

2.2. Characterization

X-ray diffraction (XRD) data on the phase composition of $MgAl(Sn)$-CO_3 and $MgAl(Sn)$-$PtCl_6$ layered hydroxides and the corresponding oxide phases were obtained on a D8 Advance (Bruker) X-ray diffractometer (CuK_α radiation, $\lambda = 1.5418$ Å) by scanning with a step of 0.05^o and accumulation time of 5 s/step at 2θ diffraction angles between 5 and 80^o.

Conditions of the oxide phase formation were found with the use of TG-DTA (thermogravimetry – differential thermal analysis). The measurements were carried out on a STA-449C Jupiter (Netzsch) device in dynamic mode using an argon medium with a rate of sample heating of 10 degrees per minute.

The nitrogen adsorption-desorption isotherms at 77.4 K were measured using an ASAP-2020 (Micromeritics) static volumetric apparatus. Prior to measurements, the samples were evacuated at 573 K for 6 hours. A range of equilibrium relative pressures was between 10^{-3} and 0.996 P/P_0. The BET specific surface area (S_{BET}) was calculated from the adsorption isotherm at equilibrium relative values of nitrogen vapor $P/P_0 = 0.05$-0.25. The adsorption pore volume (V_{ads}) was determined from the amount of nitrogen adsorbed at $P/P_0 = 0.990$. The mean pore diameter was estimated as $D = 4V_{ads}/S_{BET}$.

The measurements of carbon dioxide adsorption were made on a Sorptomatic-1900 automated static vacuum apparatus. Before measurements, the samples were treated in a vacuum (10^{-2} mm Hg) at 573 K. The isotherm of carbon dioxide adsorption obtained at P = 1 atm and a temperature of 303 K was used to calculate the total capacity of a sample with respect to

physically and chemically adsorbed CO_2. After that, the sample was evacuated to 10^{-2} mm Hg at the same temperature for 1 hour to remove physically adsorbed molecules, and the second isotherm was obtained. The difference between two isotherms in the amount of adsorbed CO_2 made it possible to determine the CO_2 amount that was retained on the surface due to its chemical features [48]. To assess the strength of basic sites, they were evacuated at 373, 473, and 573 K.

The reduction dynamics of the oxidized platinum species supported on mixed oxides Pt/MgAl(Sn)O_x was studied by the temperature-programmed reduction (TPR) on an AutoChem-2920 (Micromeritics) chemisorption analyzer. The samples obtained by calcination of LDH with the anchored platinum chloride complexes in air at 823 K were employed for TPR. TPR was carried out up to 823 K with a 10°C/min ramp rate using a 10% vol. H_2–Ar gas mixture (a flow rate of 30 mL/min). Platinum dispersion in the reduced samples was estimated by pulse chemisorption of H_2 and CO probe molecules at room temperature assuming the stoichiometry of [Pt] : [H] = 1:1, [Pt] : [CO] = 1:1.

Samples of the platinum catalysts were examined by transmission electron microscopy (TEM). TEM images were obtained on a JEM-2100 (JEOL Ltd.) electron microscope. Local Energy Dispersive X-ray (EDX) microanalysis was made on an Inca-Xact (Oxford Instruments) analyzer. Semi-quantitative calculations of the compositions were made using the software support of the analyzer. The samples were prepared by depositing the ethanol suspension of the powdered samples on a copper grid that was covered with a thin perforated carbon film. More than 100 different particles visible on the micrographs were employed to estimate the average particle size. The arithmetic mean particle diameter, d, was calculated by the following equation:

$$d = \frac{\sum n_i d_i}{\sum n_i},$$

where n_i is the frequency of the catalyst particles the diameter of size d_i.

X-ray photoelectron spectra (XPS) were recorded using a SPECS (Germany) spectrometer equipped with several isolated vacuum chambers for fast loading of samples, their thermal treatment and analysis. Samples were transferred between the chambers so as to prevent air contact. Photoelectron spectra of the samples were reproduced in the analyzer chamber at a pressure of 5×10^{-9} Torr. For each sample, spectra were recorded using MgK_α ($h\nu$ = 1253.6 eV) and AgL_α ($h\nu$ = 2984.3 eV) irradiation. The binding energy scale of spectrometer was calibrated against the lines of metallic gold and copper, Au4$f_{7/2}$ = 84.0 eV and Cu2$p_{3/2}$ = 932.6 eV. For any irradiation, the spectra of non-conducting samples were calibrated against the C1*s* line whose binding energy was taken equal to 284.8 eV. Before measurements, the samples were pre-

reduced in a hydrogen stream using a special quartz reactor and then transferred to a spectrometer in a short-term contact with air.

X-ray absorption measurements were performed at the beamline BM20 of the European Synchrotron Radiation Facility (Grenoble, France). The energy of the X-ray incident beam was selected using the reflection from a pair of water-cooled Si(111) crystal monochromators. The rejection of higher harmonics was achieved by two Si mirrors with a Rh-coating for PtL_3 edge measurements and a Pt-coating for SnK edge measurements. The energy calibration was performed using the Pt and Sn metal foil samples. The spectra at the PtL_3- and SnK-edges were obtained in the transmission mode at room temperature. The local environments of Pt and Sn atoms were simulated for the data filtered by the Fourier method (ΔR = 1–3.8 Å for PtL_3 and ΔR = 0.8–3.2 Å for SnK) with k^2 weighting ($k^2\chi(k)$) within the wave vector range of $\Delta k = 2 - 11$ Å^{-1} for PtL_3 EXAFS spectra and $\Delta k = 3 - 14$ Å^{-1} for SnK EXAFS spectra using the EXCURV 98 program. In data processing, the phase and amplitude characteristics were calculated in the von Bart and Hedin approximation. The Debye-Waller factors were equalized for O and Cl atoms and metal Pt and Sn atoms. The error in determining the interatomic distances was ± 1%, and coordination numbers, ± 10%.

2.3. Condition of propane and n-decane dehydrogenation

Dehydrogenation of propane was carried out in a flow-type reactor with a stationary catalyst bed (a 0.5 g loading) at a temperature of 863 K, atmospheric pressure, molar ratio H_2/C_3H_8 = 0.25, and weight hourly space velocity of 8 g/(g_{cat}·h). Conditions of the catalyst pretreatment included calcination in air at 823 K and reduction in flowing hydrogen at 823 K. The time of each experiment was 5 h. The composition of products was analyzed on-line using a Khromos GH-1000 gas chromatograph equipped with an Rt-Alumina PLOT column.

n-Decane dehydrogenation was carried out in a flow-type reactor with a stationary catalyst bed (a 0.5 g loading) at a temperature of 733 K, 0.18 MPa pressure, molar ratio H_2/n-decane = 7, and weight hourly space velocity of 17 g/(g_{cat} h). The composition of products was analyzed on-line using a Tsvet-800 chromatograph equipped with a PONA/PIONA column and a flame ionization detector. In the course of n-decane conversion, the groups of products were monitored, which were represented by C_1–C_8 alkanes (cracking products), isodecanes (iso-C_{10}), n-decenes (C_{10} olefins), and diolefins (C_{10} dienes). The n-decenes were a mixture of linear olefins with different double bond positions. No aromatic hydrocarbons formed under the above-specified conditions.

Before catalytic testing, all the samples were reduced at a temperature of the corresponding reaction.

3. Results and discussion

3.1. Properties of MgAl(Sn) LDH and the corresponding mixed oxides

Coprecipitation is conventionally used for the synthesis of LDH and provides high efficiency and purity of the resulting products [29-31]. In this study, coprecipitation of magnesium, tin, and aluminum hydroxides led to the formation of LDH with a variable tin content. The tin fraction in the cations with +3 and +4 charges ($Sn^{4+}/(Sn^{4+}+Al^{3+})$) changed in a wide range, while the atomic ratios $Mg^{2+}/(Al^{3+}+Sn^{4+})$, which determine to a great extent the acid-base properties of the supports based on LDH, were equal to 3. The elemental composition of the obtained samples is given in Table 1.

According to XRD, the introduction of tin cations Sn^{4+} into aluminum-magnesium LDH does not destroy the layered structure: XRD patterns of all the obtained LDH samples have a series of the 003 and 006 basal reflections as well as the peaks of {0kl} family: 012, 015, 018; {hk0}: 110, and the 113 peak (Fig. 1a), which corresponds to hydrotalcite structure (# 22-700, ICDD, PDF-2). This structure is present in the entire range of $Sn^{4+}/(Sn^{4+}+Al^{3+})$ ratios, even with the complete replacement of aluminum with tin. However, at a high content of tin $Sn^{4+}/(Sn^{4+}+Al^{3+}) > 0.1$ and an additional phase of magnesium hydroxostannate $MgSn(OH)_6$ (HSM) appears. This phase is well crystallized, and the intensity of reflections grows with the increase in tin content. The incorporation of tin cations Sn^{4+} into the hydroxide layers is confirmed by changes in the structural characteristics of LDH, namely, in the lattice parameters *a* and *c* (Table 1). The replacement of some aluminum cations Al^{3+} (ionic radius 0.0535 nm) with larger Sn^{4+} cations (ionic radius 0.0690 nm) produces a monotonic increase in parameter *a*, the value of which is determined by the distance between cations in brucite-like layers ($a = 2d_{110}$), from 0.3066 to 0.3143 nm. It is known that the lattice parameter *c* ($c = 3d_{003}$) depends on the nature, size and concentration of the interlayer anions, and the hydration degree of the material. In the considered series of samples synthesized under identical conditions, the decrease in this parameter from 2.352 to 2.316 nm with the increasing content of tetravalent tin cation is caused by strengthening the interaction (attraction) between positively charged brucite-like layers and the interlayer space. Thus, the analysis of structural characteristics shows that under the chosen conditions of synthesis the samples containing the individual phase MgAl(Sn)-LDH can be obtained only at a limited tin content. At the same time, even in the absence of aluminum cations, the synthesis of LDH containing Mg^{2+} and Sn^{4+} cations is possible.

In the formation of the oxide phase, thermal decomposition of the tin-containing LDH as well as the magnesium-aluminum samples occurs in two steps: the low-temperature region (below 473 K) corresponds to the removal of interlayer water, and the high-temperature region

(above 723 K) is related to dehydroxylation of the layers and removal of the interlayer anions (Fig. 1S). The appearance of additional weight loss peaks in the region of 533 K with increasing tin content is caused by decomposition of the HSM phase and agrees with the XRD data [44].

XRD patterns of the LDH samples calcined at 823 K (Fig. 1b) show the peaks that are often attributed in the literature to the periclase-like MgO phase with the face-centered cubic lattice [49]. At the same time, earlier it was found [50] that the structure of the obtained mixed oxide is a layered defective spinel (s.g. Fd3m). The lattice parameters were specified in [50] when examining the structure of the mixed oxide as the periclase-like one in the space group Fm3m. The analysis of lattice parameters of the calcined samples (Table 1S) revealed the monotonic growth of the lattice constant *a* from 0.4191 to 0.4460 nm with increasing fraction of Sn^{4+}, the growth being related to the difference in the ionic radii of Sn^{4+} and Al^{3+} in the oxide structure. In addition, calcination of the LDH samples containing the impurity HSM phase with $Sn^{4+}/(Sn^{4+}+Al^{3+} > 0.1)$ leads to the formation of minor amounts of the tetragonal tin oxide SnO_2 (Fig. 1b, Table 1S). The presence of magnesium ions in this structure is hard to detect due to close sizes of the cations.

It was found that tin introduction into the mixed oxides does not affect their unique ability to restore the layered structure during rehydration ("the memory effect") [29-31, 51] (Fig. 1c). When the mixed oxide contacts water (the formation of the "activated form" of LDH [31, 47]), primarily the hydroxide ions are present in the interlayer space. This leads to a decrease in the interlayer distance in the obtained LDH as compared with LDH of the same cationic composition containing the interlayer carbonate-ions, and to the corresponding decrease in the lattice parameter *c* from 2.342 to 2.328 nm.

The textural properties of the mixed oxides obtained by calcination of LDH are important for their further use as the catalyst supports. Investigation of the main parameters of the $MgAl(Sn)O_x$ pore structure showed (Table 2) that the aluminum-magnesium sample has the largest specific surface area (230 m^2/g). As the tin fractions increases, the specific surface area, adsorption volume and mean pore diameter decrease monotonically. This result is consistent with the data reported in [44]. However, when aluminum is completely replaced with tin, the obtained sample containing $MgSnO_x$ with the minimum S_{BET} is characterized by higher adsorption volume and mean pore diameter as compared with the samples containing three cations. The analysis of pore size distribution curves (PSDC) showed (Fig. 2) that changes in the chemical composition of oxides lead to rearrangement of their porous space. The samples containing bimetallic systems $MgSnO_x$ and $MgAlO_x$ typically have a wide pore size distribution with a significant contribution of 10-80 nm mesopores, whereas at simultaneous presence of three metals a narrower pore size distribution is observed with the prevalence of pores with the

diameter less than 20 nm. It should be noted that the observed differences in the textural characteristics of oxide phases may be caused not only by different composition of the corresponding hydroxide precursors (LDH), but also by the presence of the thermal decomposition product of the impurity HSM phase, the amount of which grows with the tin content (Fig. 1b).

Along with the textural characteristics, the acid-base properties of oxide supports are also important. In high-temperature dehydrogenation reactions, the use of non-acid supports decreases the intensity of coking and inhibits fast deactivation of the catalysts. The aluminum-magnesium oxides are characterized by rather strong basic properties [30]; however, there such information is absent for the tin-containing analogs. Earlier [41, 52], we employed the static method for determining the adsorption capacity for carbon dioxide to evaluate basic properties [48]. The application of this method to estimate the effect of tin introduction on basicity of the tin-containing samples showed (Fig. 3) that partial or even complete replacement of Al by Sn does not lead to a decrease in basicity but, on the contrary, increases the number of basic sites, both weak, from which CO_2 is desorbed at lower temperatures [48], and the sites of strong CO_2 chemisorption able to keep these test molecules even at 473 K.

3.2. The formation and properties of supported platinum

To synthesize platinum catalysts, MgAl(Sn)O_x mixed oxides were immersed in an aqueous solution of chloroplatinic acid. During rehydration, the formation of the activated LDH form containing the interlayer OH^- ions was accompanied by intercalation of platinum complexes in the interlayer space of the forming LDH [29, 53-55]. As a result, at a constant cationic composition of hydroxide layers, the interlayer distance increased as compared to LDH without complex anions. For instance, for the sample with Sn/(Sn+Al) = 0.1 (Fig. 1c), the lattice parameter *c* changed in the following sequence: 2.342 nm (MgAl(Sn0.1)-CO_3) – 2.328 nm (MgAl(Sn0.1)-OH) – 2.357 nm (MgAl(Sn0.1)-([$PtCl_6$]+OH), 1 wt% Pt). This type of platinum anchoring provides the maximum interaction of metal complex with the support, and in the presence of Sn^{4+} in cationic layers, a stronger Coulombic interaction between anionic complexes and hydroxide layers.

For the further formation of the Pt/MgAl(Sn)O_x catalyst, LDH samples with the anchored platinum complexes were oxidized and reduced. The data of temperature-programmed reduction of the samples after calcination at 823 K show (Fig. 4a) that the presence of tin in the support strongly affects the hydrogen consumption process. As Sn content grows, hydrogen consumption increases in the high-temperature area, which may be related to the partial reduction of tin. When Sn/(Sn+Al) = 0.7, this process gains intensity, the regions of tin and platinum reduction overlap, and the amount of adsorbed hydrogen significantly exceeds the value necessary for platinum

reduction from its oxides (Table 2S). It is likely that the presence of platinum (the reduction of which occurs at a lower temperature of 473-543 K) activates the process of tin reduction. This effect was noted earlier [56], when the onset temperature of tin reduction dropped from 823 to 503 K in the presence of platinum.

The partial reduction of tin is confirmed by the further detailed study of Pt/MgAl(Sn)O_x samples. Thus, the XRD pattern of the 1%Pt/MgAl(Sn0.7)O_x sample (Fig. 4b) shows the peaks of the metallic tin phase; structural characteristics of all the identified phases in the reduced samples are listed in Table 3S. Since the supported platinum is able to activate the reduction of adjacent tin ions, a part of tin is removed from the support structure, which is accompanied by a decrease in the lattice constant of the mixed oxide. For example, the reducing treatment of the 1%Pt/MgAl(Sn0.7)O_x sample decreases the lattice constant of the mixed oxide phase from 0.4239 to 0.4225 nm. The observed changes in the Sn*K*-XANES spectra of 1%Pt/MgAl(Sn)O_x samples (Fig. 2S) agree well with the data of other methods on the tin reduction: the mean positive charge on Sn atoms decreases successively upon transition from the sample with Sn/(Sn+Al) = 0.1 to samples with Sn/(Sn+Al) = 0.3 and 0.7. Modeling of Sn*K* EXAFS spectra (Fig. 4S) shows that an increase in the tin content is accompanied by a decrease in the number of Sn-O bonds and an increase in N(Sn) from 3.2 to 4.1 (Table 3).

Analysis of the $Sn3d_{5/2}$ line in XP spectra allowed us to identify the oxidized and reduced tin species and estimate their ratio. Deconvolution of the XP spectrum revealed the states with the binding energies of 485.0 and 487.0 eV (Fig. 5a, Table 4) corresponding to metallic and oxidized tin. Unfortunately, XPS cannot discriminate Sn(II) from Sn(IV) due to small differences in the binding energies [57]. It was found that noticeable amounts of the reduced tin species are formed at Sn/(Sn+Al) > 0.1, and their fraction in the total amount of tin on the surface of 1%Pt/MgAl(Sn-0.3)O_x and 1%Pt/MgAl(Sn-0.7)O_x samples reaches 50 at.%. It is known that the interaction of Sn(0) with reduced platinum can produce alloys of various compositions. The formation of Sn(0) upon reduction of PtSn catalysts under mild conditions indicates the interaction between the metals and is usually observed when the catalysts are synthesized using platinum-tin complexes.

Despite the observed difference in the electronic states, tin is distributed quite uniformly in the reduced samples (Fig. 4S). Elemental analysis of the samples by energy-dispersive X-ray spectroscopy in the TEM study showed that the uniform distribution is typical also of the other components of the catalysts (O, Mg, Al, Pt). Only in the samples with Sn/(Sn+Al) $\geq$ 0.3 it is possible to find some areas enriched with tin; their formation may be related with the presence of the side HSM phase in the synthesized LDH.

Estimation of the platinum particle size by TEM revealed a noticeable decrease in their mean diameter upon introduction of tin; for example, a comparison of 1%Pt/$MgAlO_x$ and 1%Pt/MgAl(Sn-0.1)O_x samples (Fig. 6) showed that their mean diameter diminished from 3.0 to 2.2 nm. Unfortunately, we failed to obtain contrast images of platinum particles when analyzing the samples with high tin content. A similar effect was observed in our earlier study on the modifying effect of zinc introduced into the LDH structure [41]. In this case, the chemisorption method cannot be used as an alternative for determining the dispersion of the supported metal, since it is non-informative for investigation of Pt/MgAl(M)O_x catalysts due to modification of the electronic properties of platinum with the use of magnesium-containing supports [41, 58, 59]. The introduction of tin into the mixed oxide led to further deterioration of the adsorption properties of platinum with regard to the test molecules (Table 2S). Thus, the mean size calculated from the chemisorption data (by equation $D_{chem} = 6V/S$, where V is the volume of Pt atom, and S is the platinum surface) was 7.5 nm for the 1%Pt/$MgAlO_x$ sample and 28 nm for 1%Pt/MgAl(Sn-0.1)O_x. Similarly, in [60] a decrease in the amount of chemisorbed H_2 and CO molecules with increasing Sn/Pt ratio was observed; this effect is not related to changes in the size of platinum particles.

At the same time, the TEM data on the growth of dispersion of supported platinum in the tin-containing catalysts agree well with the XPS data . As the tin content increases, the intensity of the $Pt3d_{5/2}$ line in the XP spectrum also increases (Fig. 5b), which usually correlates with the number of available platinum atoms on the sample surface [61]. Therewith, the atomic ratio Pt/Mg grows monotonically (Table 4).

The EXAFS study was carried out to determine the structural parameters of platinum particles in 1%Pt/MgAl(Sn)O_x catalysts. Figure 5S displays PtL_3 EXAFS spectra and radial distribution functions of 1%Pt/MgAl(Sn)Ox samples with Sn/(Sn+Al) = 0.1, 0.3, 0.7. The local structure parameters (interatomic distances (R) and partial coordination numbers (N)) were determined in the simulation process by fitting of EXAFS data (Table 5) under the assumption that the platinum atoms are in contact with each other, with oxygen and chlorine atoms and possibly with tin atoms. Analysis of the obtained data (Table 5) shows that tin introduction in the support produces noticeable changes in the structure of the catalyst metal sites. First of all, as the tin content grows, the number of Pt-Pt bonds decreases monotonically, which agrees well with the TEM data on the decrease in the size of platinum particles in Sn-containing samples. In addition, tin atoms are present in the coordination sphere of all the studied samples. However, in the 1%Pt/MgAl(Sn-0.1)O_x sample, where the reduced tin species were not found, the coordination number of tin is only 0.5, whereas N(Sn) reaches 4 as the tin content in the support increases. It should be noted that the Pt-Sn distance obtained by simulation of EXAFS spectra

for platinum is higher (0.303 or 0.311 nm) than the corresponding distance typical of the Pt-Sn solid solutions (0.273 – 0.286 nm) [63], which could be explained by the presence of oxygen and chlorine in the coordination sphere of platinum, and probably excludes the formation of PtSn solid solutions and alloys in the studied samples. The presence of the Pt-O bond with N(O) close to 1 may indicate both the the oxidized state of a part of platinum and the possible interaction of metal with the oxide support [64]. Chlorine in the coordination sphere of platinum in all the studied catalysts is the decomposition product of the precursor compound $H_2[PtCl_6]$. The increase in the number of Pt-Cl bonds with increasing the tin content in the samples can be a result of a stronger interaction of the anionic chloride complexes with the hydroxide layers, the charge of which increases with the growing number of Sn^{4+} cations in the LDH structure.

XPS was used to obtain data on the state of supported platinum in the catalysts synthesized with the use of Sn-containing LDH. The study was performed using the AgL_α source with $h\nu$ = 2984.3 eV, which solved the problem of mutual overlapping of Pt4f and Al2p lines of the active component and support when using X-ray tubes with Al or Mg anodes. In the obtained XPS spectra, most intensive is the Al1s line with the binding energy $E_b \approx 1560$ eV. Therewith, monochromatization strongly decreases the halfwidth of the initially broad AgL_α line and allows a reliable interpretation of the electronic state of platinum: for metal E_b = 2121.8 eV; for Pt^{2+} (K_2PtCl_4) E_b = 2123.5 eV; and for Pt^{4+} (K_2PtCl_6) E_b = 2125 eV [65]. The atomic ratios of elements were calculated using the reference data reported in [66]. Analysis of the $Pt3d_{5/2}$ line for the studied samples showed that at different tin contents the spectrum is identical to that obtained earlier for platinum deposited on the aluminum-magnesium support [41, 46,]; this indicates that all the samples contain mostly the metallic platinum. At the same time, a shift of the maximum of the $Pt3d_{5/2}$ line to lower energies with increasing platinum dispersion admits the existence of electronic interactions accompanied by charge transfer from the Sn-containing support to platinum. Such interaction may lead to the observed decrease in chemisorption of the H_2 and CO test molecules. The authors of [67] analyzed the $Pt4f_{7/2}$ line and observed a 0.3-1.0 eV shift of the binding energy towards lower energies with increasing tin content in PtSn/C bimetallic catalysts; this shift was attributed to differences in electronegativity of the elements, namely, to the charge transfer from less electronegative tin to more electronegative platinum.

To reveal the effect of tin in the oxide support on the catalytic properties of supported platinum, the reactions of propane and n-decane dehydrogenation were used. The chosen reaction conditions (moderate temperature and high dilution with hydrogen) made it possible to avoid fast deactivation of the catalysts, evaluate the dehydrogenating activity of platinum, and compare the catalysts without approaching the equilibrium conversions of the selected alkanes [4, 6]. Platinum content in the catalysts, 0.3 wt%, was close to industrial values. As seen from

the dependences in Fig. 7, the introduction of tin into support exerts a substantial effect on dehydrogenating properties of the platinum sites: the conversion of both compounds extremely depends on the tin content in the support.

Figure 7 displays the propane conversions and selectivities of propylene formation after 4 h of the catalyst operation. The presented dependence suggests that the increase in the catalyst activity results from the tin addition within a narrow range of concentrations comparable with the content of supported platinum and corresponding to the ratio Sn/(Sn+Al) = 0.002-0.01. The introduction of the minimum amount of tin can produce more than a twofold increase in the propane conversion. It should be noted that the growth of conversion is not accompanied by a decrease in the selectivity of propylene formation. This effect is probably may be caused by an increase in the number of active sites of a similar nature. A higher tin content in the support leads to deactivation of the catalyst.

A similar tendency is observed when the catalysts are tested in dehydrogenation of n-decane. The activity of samples with the ratio Sn/(Sn+Al) = 0.005-0.05 significantly exceeds that of samples without tin. Analysis of the reaction products composition showed (Fig. 6S) that introduction of tin modifies the properties of both platinum and the support. A decrease in the catalyst activity toward the formation of cracking and isomerization products and agrees with the established (Fig. 3) higher basicity of the Sn-containing oxide support. The decreased yield of dienes results from weakening of the bond between platinum sites and the target products of the reaction – decenes, which promotes their desorption and prevents further dehydrogenation.

CONCLUSION

Although the catalytic system $Pt/MgAlO_x$ obtained with the use of aluminum-magnesium LDH is promising for dehydrogenation of alkanes and tin is considered to be one of the most efficient modifiers of the platinum properties in the existing dehydrogenation catalysts , there is no information on the application of Sn-containing LDH as the supports for catalysts for reactions of this type. First of all, this is related to the limited information on the synthesis and structure of Sn-containing LDH and their transformations at different steps of the catalyst synthesis. This is why in our study the emphasis was made on the synthesis of Sn-containing LDH with a wide variation of tin concentration. It was shown that the chosen conditions of the synthesis make it possible to obtain the phase-uniform systems with the Sn/(Sn+Al) ratio up to 0.1. A partial replacement of aluminum atoms with tin does not change high specific surface areas of the mixed oxides equal to 150-200 mg^2/g and basic properties of the surface.

In addition, it was shown for the first time that the Sn-containing mixed oxides are able to restore the initial layered structure during hydration in water (“the memory effect”), which

allows intercalating the anionic platinum complexes into the interlayer space of the forming LDH and provides a strong interaction of the metal complex with the support. As a result, the platinum sites formed in the reducing atmosphere initiate the reduction of a part of tin at temperatures below 723 K.

Independent TEM, EXAFS and XPS studies revealed increase in the dispersion of supported platinum with the introduction of tin into support. Therewith, no significant electronic effects were observed (positions of the $Pt3d_{5/2}$ line for all Sn-containing samples are nearly identical and close to the binding energy for Pt(0)) although the absence of a noticeable amount of oxidized platinum species on the surface of highly dispersed particles may be caused by electronic interactions between platinum and $MgAl(Sn)O_x$ support with donation of electron density to the particles of supported metal.

It was established that the growth of alkane conversion at the retained high formation selectivity of the corresponding alkenes is observed within the narrow interval of Sn/Pt = 1-2. The high Sn/Pt ratio initiates the intensive reduction of tin and leads to a decrease in the catalyst activity.

The growth of platinum dispersion and dehydrogenating activity upon tin introduction in the support may be caused by an increase in the interaction strength between metal complex and support at the step of anchoring the active component precursor. The introduction of Sn^{4+} cations in the hydroxide layers increases positive charge of the layers and strength of their electrostatic interaction with anion platinum complexes. This decreases mobility of the complexes in thermal activation processes, thus preventing the formation of large platinum particles.

The presented information on the structure and phase composition of the supports and catalysts based on LDH with different content of Sn as well as on the conditions for the formation of reduced tin species can be useful for designing the catalytic sites of a specified composition and interpreting the observed catalytic effects in the Sn-containing catalysts.

Acknowledgements

The authors are grateful to O.V. Maevskaya, G.G. Savel'eva, A.V. Babenko, and N.V. Antonicheva for testing the properties of the synthesized samples. Characterization of the catalysts was performed using equipment of the Omsk Regional Center of Collective Usage, Siberian Branch of the Russian Academy of Sciences. The work was carried out according to the state task of the IHP SB RAS (project registration number AAAAA17-117021450095-1). The study of Pt-containing catalysts by XPS using Ag La radiation was partly carried out according to the state task of the BIC SB RAS (project registration number AAAA-A17-117041710078-1).

References

[1] V. A. Mazzieri, J. M. Grau, J. C. Yori, C. R. Vera, C. L. Pieck, Appl. Catal., A. 354(1-2) (2009) 161 – 168.

[2] A. Erhan Aksoylu, M.M.A. Freitas, J.L. Figueiredo, Catal. Today. 62 (2000) 337 – 346.

[3] V. Ponec, Appl. Catal. A: Gen. 149 (1997) 27 – 48.

[4] J. J. H. B. Sattler, J. Ruiz-Martinez, E. Santillan-Jimenez, B. M. Weckhuysen, Chem. Rev. 114 (2014) 10613 – 10653.

[5] H. N. Pham, J. J. H. B Sattler, B. M. Weckhuysen, A. K. Datye, ACS Catal. 6(4) (2016) 2257 – 2264.

[6] A. W. Hauser, J. Gomes, M. Bajdich, M. Head-Gordon, A. T. Bell, Phys. Chem. Chem. Phys. 15(47) (2013) 20727 – 20734.

[7] S. Sahebdelfar, M.T. Ravanchi, F.T. Zangeneh, S. Mehrazma, S. Rajabi, Chem. Eng. Res. Des. 90 (2012) 1090 – 1097.

[8] Z. Nawaz, X. Tang, Q. Zhang, D. Wang, W. Fei, Cat. Commun. 10 (2009) 1925 – 1930.

[9] L.S. Carvalho, P. Reyes, G. Pecchi, N. Figoli, C.L. Pieck, M.C. Rangel, Ind. Eng. Chem. Res. 40 (2001) 5557 – 5563.

[10] R.D. Cortright, J.M. Hill, J.A. Dumesic, Catal. Today. 55 (2000) 213 – 223.

[11] Z. Paa´l, A. Gyory, I. Uszkurat, S. Olivier, M. Gue´rin, C. Kappenstein, J. Catal. 168 (1997) 164 – 175.

[12] C. Kappenstein, M. Gue´rin, K. La´za´r, K. Matusek, Z. Paa´l, J. Chem. Soc., Faraday Trans. 94 (1998) 2463 – 2473.

[13] W. S. Yang, L. W. Lin, Y. N. Fan and J. L. Zang, Catal. Lett. 12 (1992) 267 – 275.

[14] R. Burch, L. C. Garla, J. Catal. 71 (1981) 360 – 372.

[15] M.L. Casella, G.J. Siri, G.F. Santori, O.A. Ferretti, M. Ramı´rez de Agudelo, Langmuir 16 (2000) 5639 – 5643.

[16] C. Ve´rtes, E. Ta´las, I. Czako´-Nagy, J. Ryczkowski, S. Go¨bo¨lo¨s, A. Ve´rtes, J. Margitfalvi, Appl. Catal. 68 (1991) 149 – 159.

[17] J. Llorca, N. Homs, J. Leo´n, J. Sales, J.L.G. Fierro, P. Ramı´rez de la Piscina, Appl. Catal., A. 189 (1999) 77 – 86.

[18] K. Balakrishnan, J. Schwank, J. Catal. 138 (1992) 491 – 499.

[19] M.C. Roma´n-Martı´nez, D. Cazorla-Amoro´ s, H. Yamashita, S. de Miguel, O.A. Scelza, Langmuir 16 (2000) 1123 – 1131.

[20] C. Audo, J.F. Lambert, M. Che, B. Didillon, Catal. Today 65 (2001) 157 – 162.

[21] L. Bednarova, C.E. Lyman, E. Rytter, A. Holmen, J. Catal. 211 (2002) 335 – 346.

[22] G.T. Baronetti, S.R. Miguel, O.A. Scelza, M.A. Fritzler, A.A. Castro, Appl. Catal. 19 (1985) 77 – 85.

[23] G. T. Baronetti, S. R. de Miguel, O. A. Scelza, A. A. Castro, Appl. Catal. 24 (1986) 109 – 116.

[24] F. Humblot, J.P. Candy, F. Lepeltier, B. Didillon, J.M. Basset, J. Catal. 179 (1998) 459 – 468.

[25] V. Gertosio, C.C. Santini, M. Taoufik, F. Bayard, J.M. Basset, J. Buendia, M. Vivat, J. Catal. 199 (2001) 1 – 8.

[26] H. Zhu, D. H. Anjum, Q. Wang, E. Abou-Hamad, L. Emsley, H. Dong, P. Laveille, L. Li, A. K. Samal, J.-M. Basset, J. Catal. 320 (2014) 52 – 62.

[27] Y. W. Zhang, Y. M. Zhou, J. J. Shi, S. J. Zhou, X. L. Sheng, Z. W. Zhang, S. M. Xiang, J. Mol. Catal., A: Chem. 381 (2014) 138 – 147.

[28] S. Bocanegra, A. Ballarini, P. Zgolicz, O. Scelza, S. de Miguel, Catal. Today 143 (2009) 334 – 340.

[29] E. Conterosito, V. Gianotti, L. Palin, E. Boccaleri, M. Milanesio, Inorg. Chim. Acta 470, 30 (2018) 36 – 50.

[30] J. Feng, Y. He, Y. Liu, Y. Du, D. Li, Chem. Soc. Rev. 44 (2015) 5291 – 5319.

[31] O. B. Belskaya, N. N. Leont'eva, T. I. Gulyaeva, V. A. Drozdov, V. P. Doronin, V. I. Zaikovskii, V. A. Likholobov, Kinet. Catal. 52(5) (2011) 761 – 769.

[32] D. Akporiaye, M. Roennekleiv, P. Hasselgaard, (Den Norske Stats Oljeselskap AS). NO Patent 308989, 2000.

[33] A. Virnovskaia, S. Morandi, E. Rytter, G. Ghiotti, U. Olsbye, J. Phys. Chem. C. 111 (2007) 14732 – 14742.

[34] V. Galvita, G. Siddiqi, P. Sun, A.T. Bell, J. Catal. 271 (2010) 209 – 219.

[35] J. Wu, Z. Peng, A.T. Bell, J. Catal. 311 (2014) 161 – 168.

[36] P. Sun, G. Siddiqi, M. Chi, A.T. Bell, J. Catal. 274 (2010) 192 – 199.

[37] G. Siddiqi, P. Sun, V. Galvita, A.T. Bell, J. Catal. 274 (2010) 200 – 206.

[38] P. Sun, G. Siddiqi, W.C. Vining, M. Chi, A.T. Bell, J. Catal. 282 (2011) 165 – 174.

[39] J. Wu, Z. Peng, P. Sun, A.T. Bell, Appl. Catal., A. 470 (2014) 208 – 214.

[40] S. Fang, K. Zhang, C. Wang, L. Ma, Q. Zhang, Q. Liu, L. Chen, L. Chen, Q. Zhang, Z. Tian, RSC Adv. 7 (2017) 22836 – 22844 .

[41] O.B. Belskaya, L.N. Stepanova, T.I. Gulyaeva, S.B. Erenburg, S.V. Trubina, K. Kvashnina, A.I. Nizovskii, A.V. Kalinkin, V.I. Zaikovskii, V.I. Bukhtiyarov, V.A. Likholobov, J. Catal. 341 (2016) 13 – 23.

[42] X. Zheng, P. A. Cusack, Fire Mater. 37 (2013) 35 – 45.

[43] O. Saber, J. Phys. Conf. Ser. 61 (2007) 825 – 830.

[44] S. Velu, K. Suzuki, T. Osaki, F. Ohashi, S. Tomura, Materials Research Bulletin, 34(10/11) (1999) 1707 – 1717.

[45 63] O. B. Belskaya, L. N. Stepanova, T. I. Gulyaeva, N. N. Leont'eva, V. I. Zaikovskii, A. N. Salanov, V. A. Likholobov, Kinet. Catal. 57(4) (2016) 546 – 556.

[46] O.B. Belskaya, T.I. Gulyaeva, V.P. Talsi, M.O. Kazakov, A.I. Nizovskii, A.V. Kalinkin, V.I. Bukhtiyarov, V.A. Likholobov, Kinet. Catal. 55(6) (2014) 786 – 792.

[47] O.B. Belskaya, V.P. Doronin, V.A. Likholobov, Kinet. Catal. 52(6) (2011) 876 – 885.

[48] R. Salvador, B. Casal, M. Yates, M.A. Martin-Luengo, E. Ruiz-Hitzky, Appl. Clay Sci. 22 (2002) 103 – 113.

[49] S. Miyata, Clays Clay Miner. 28(1) (1980) 50 – 56.

[50] S.V. Cherepanova, N.N. Leont'eva, A.B. Arbuzov, V.A. Drozdov, O.B. Belskaya, N.V. Antonicheva, J. Solid State Chem. 225 (2015) 417 – 426.

[51] N.N. Leont'eva, V.A. Drozdov, O.B. Bel'skaya, L.N. Stepanova, S.V. Cherepanova, S.V. Tsybulya, Theor. Exp. Chem. 48(4) (2012) 278 – 282.

[52] O.B. Belskaya, O.N. Baklanova, N.N. Leont'eva, T.I. Gulyaeva, V.A. Likholobov, Procedia Engineering 113 (2015) 91 – 97.

[53] N. Chubar, R. Gilmour, V. Gerda, M. Mičušík, M. Omastova, K. Heister, P. Man, J. Fraissard, V. Zaitsev, Adv. Colloid Interface Sci. 245 (2017) 62 – 80

[54] C. Yang, L. Liao, G. Lv, L. Wua, L. Mei, Z. Li, J. Colloid Interface Sci. 479 (2016) 115 – 120.

[55] R. Celis, M. Á. Adelino, B. Gámiz, M. C. Hermosín, W. C. Koskinen, J. Cornejo, Appl. Clay Sci. 96 (2014) 81 – 90.

[56] N. Yamaguchi, N. Kamiuchi, H. Muroyama, T. Matsui, K. Eguchi, Catal. Today, 164 (2011) 169 – 175.

[57] G. Neri, C. Milone, S. Galvagno, A.P.J. Pijpers, J. Schwank, Appl. Catal. A. General 227 (2002) 105 – 115.

[58] O. B. Belskaya, L. N. Stepanova, T. I. Gulyaeva, D. V. Golinskii, A. S. Belyi, V. A. Likholobov, Kinet. Catal. 56 (2015) 655 – 662.

[59] L. Bednarova, C.E. Lyman, E. Rytter, A. Holmen, J. Catal. 211 (2002) 335 – 346.

[60] T. Inoue, K. Tomishiget, Y. A. Iwasawa, J. Chem. SOC., Faraday Trans. 92(3) (1996) 461 – 467.

[61] M. Yu. Smirnov, E. I. Vovk, A. V. Kalinkin, E. Yu. Gerasimov, V. I. Bukhtiyarov, Russ. Chem. B, Int. Edition, 63(12) (2014) 2733 – 2736.

[62] Inorganic Crystal Structure Database 105852-ICSD; 105855-ICSD. http://icsdweb.fiz-karlsruhe.de

[63] Crystallography Open Database; http://www.crystallography.net

[64] S. Sakellson, M. McMillan, G.L. Haller, J. Phys. Chem. 90 (1986) 1733 – 1736.

[65] A.V. Kalinkin, M.Yu. Smirnov, A.I. Nizovskii, V.I. Bukhtiyarov, J. Electron Spectrosc. Relat. Phenom. 177 (2010) 15 – 18.

[66] J.Z. Shyu, K. Otto, Appl. Surf. Sci. 32 (1988) 246 – 252.

[67] J. H. Kim, S. M. Choi, S. H. Nam, M. H. Seo, S. H. Choi, W. B. Kim, Appl. Catal. B. 82 (2008) 89 – 102.

Figure captions

Fig. 1. XRD patterns of samples: (a) LDH MgAl(Sn)-CO_3 with various tin content, 1 – MgAl, 2 – MgAl(Sn0.1), 3 – MgAl(Sn0.3), 4 – MgAl(Sn0.7), 5 – MgSn; (b) mixed oxides MgAl(Sn)O_x with different tin content obtained after calcination of LDH at 550°C, 1 – MgAl, 2 – MgAl(Sn0.1), 3 – MgAl(Sn0.3), 4 – MgAl(Sn0.7), 5 – MgSn; (c) LDH MgAl(Sn0.1) – A^{n-} containing different interlayer anions A^{n-} = CO_3^{2-} (1), OH^- (2), $[PtCl_6]^{2-}$ (3).

Figure 1

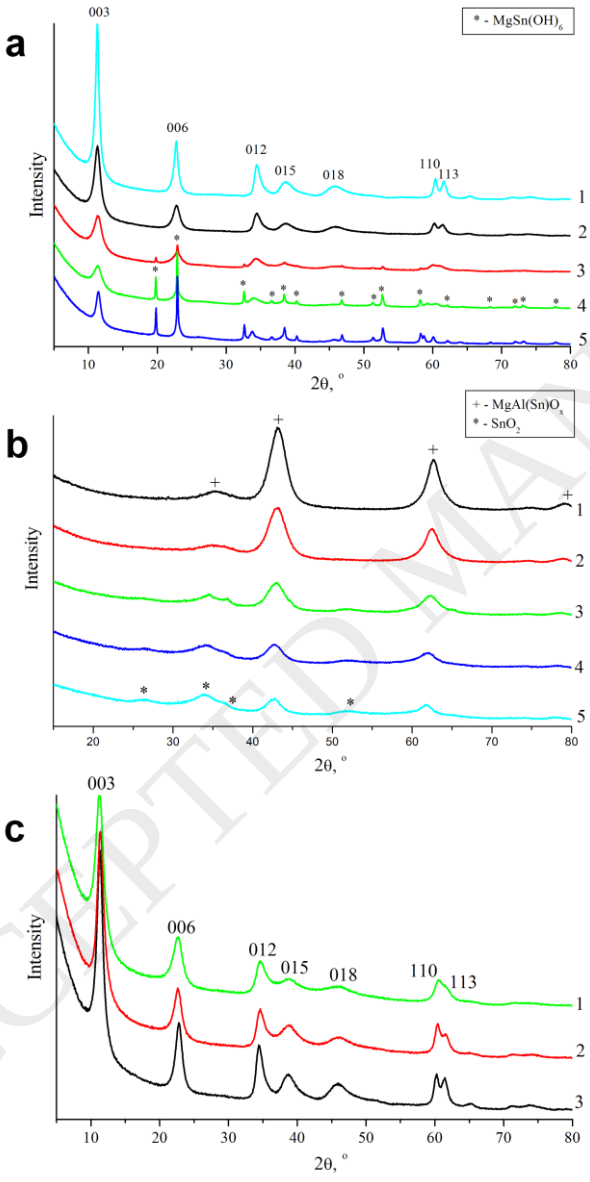

Fig. 2. Pore size distribution curves (PSDC) calculated by the BJH method from the adsorption branch for MgAl(Sn)Ox samples with the atomic ratio Sn/(Sn+Al) = 0, 0.1, 0.3, 0.7, 1.0, curves 1-5, respectively. All the samples were synthesized from MgAl(Sn)-CO_3 calcined at 823 K.

Figure 2

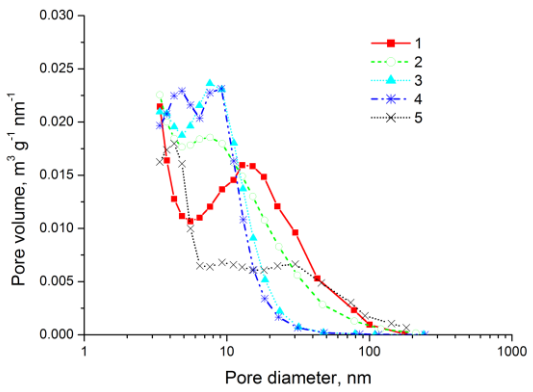

Fig. 3. The adsorption with respect to CO_2 for MgAl(Sn)Ox samples with the atomic ratio Sn/(Sn+Al) = 0, 0.1, 0.5, 0.7, 1.0, $Mg^{2+}/(Al^{3+}+Sn^{4+})$ = 3. Temperature of CO_2 adsorption was 303 K, the desorption temperature was 303 (1), 373 (2) and 473 K (3).

Figure 3

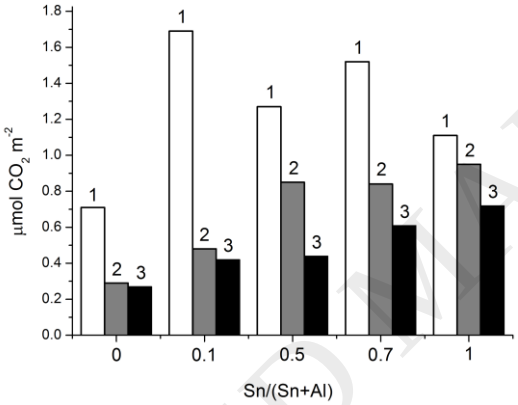

Fig. 4. TPR profiles of $PtO_x/MgAl(Sn)O_x$ (1 wt.% Pt) samples. $T(O_2)$ = 823 K with the atomic ratio Sn/(Sn+Al) = 0, 0.1, 0.3, 0.7, curves 1-4, respectively (a); XRD patterns of 1%$Pt/MgAl(Sn)O_x$ samples with the atomic ratio Sn/(Sn+Al) = 0.1, 0.3, 0.7, curves 1-3, respectively. The samples were reduced at 823 K (b).

Figure 4

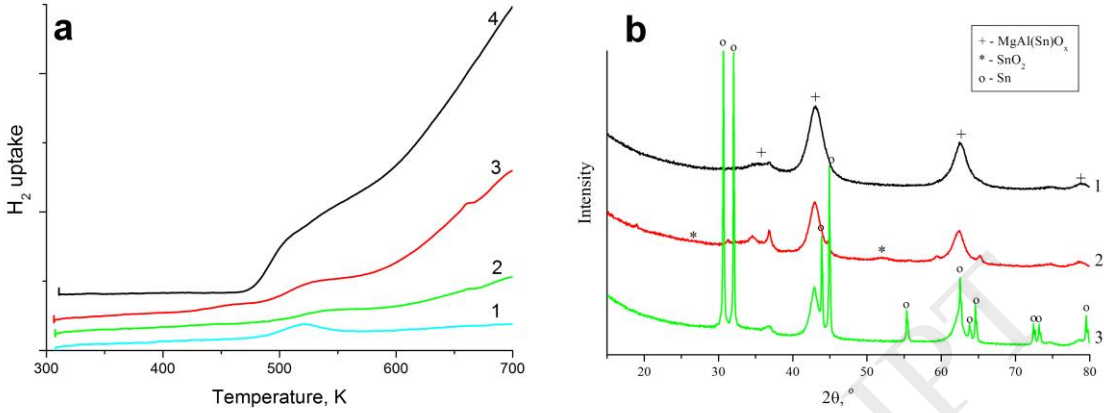

Fig. 5. Tin $Sn3d_{5/2}$ (a) and platinum $Pt3d_{5/2}$ (b) XPS spectra of 1%Pt/MgAl(Sn)O_x samples with Sn/(Sn+Al) = 0.1, 0.3, 0.7, spectra 1-3, respectively. The samples were calcined at 823 K and reduced at 823 K.

Figure 5

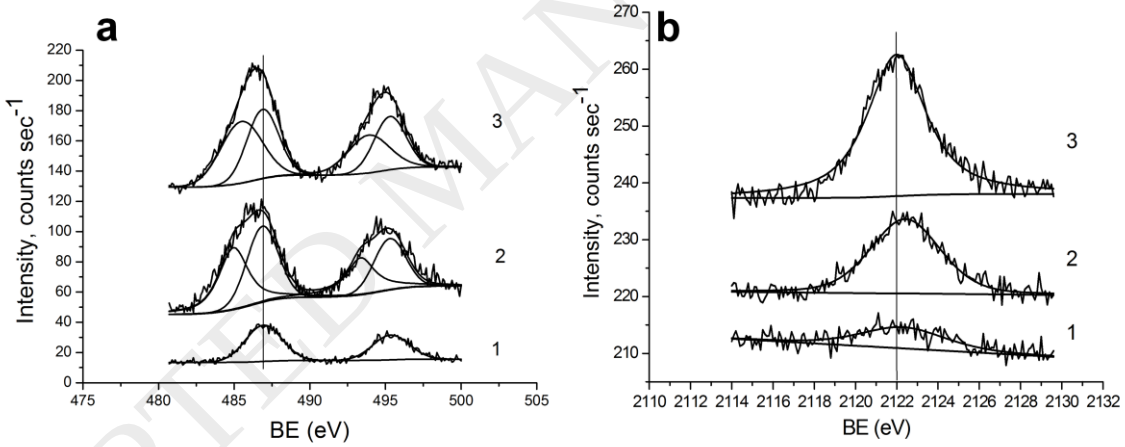

Fig. 6. TEM images and particle size distribution for 1%Pt/MgAlO_x (a) and 1%Pt/MgAl(Sn0.1)O_x (b) samples.

Figure 6

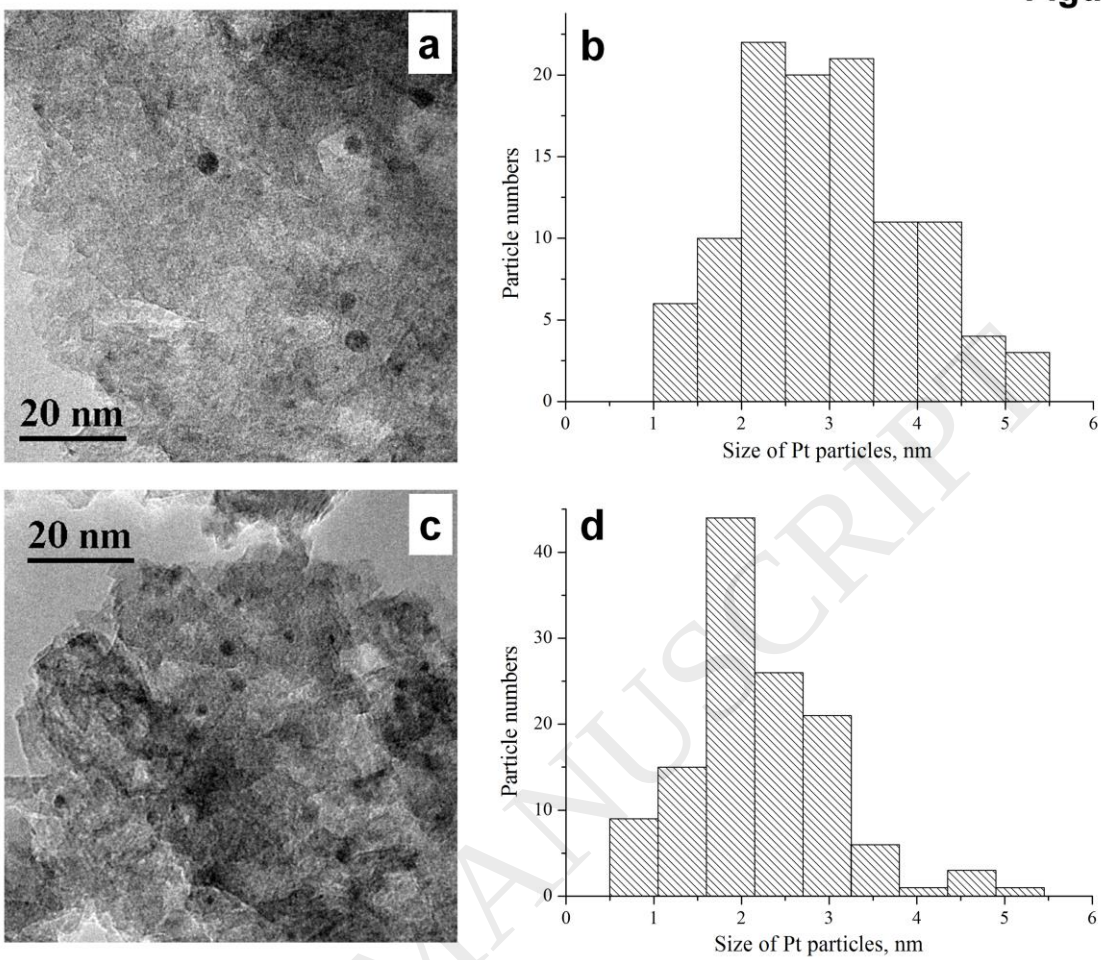

Fig. 7. Dependence of propane conversion and formation selectivity of propylene on the fraction of Sn (a); and dependence of n-decane conversion and formation selectivity of n-decenes on the fraction of Sn (b) for samples of 0.3%Pt/MgAl(Sn)O_x catalysts.

Figure 7

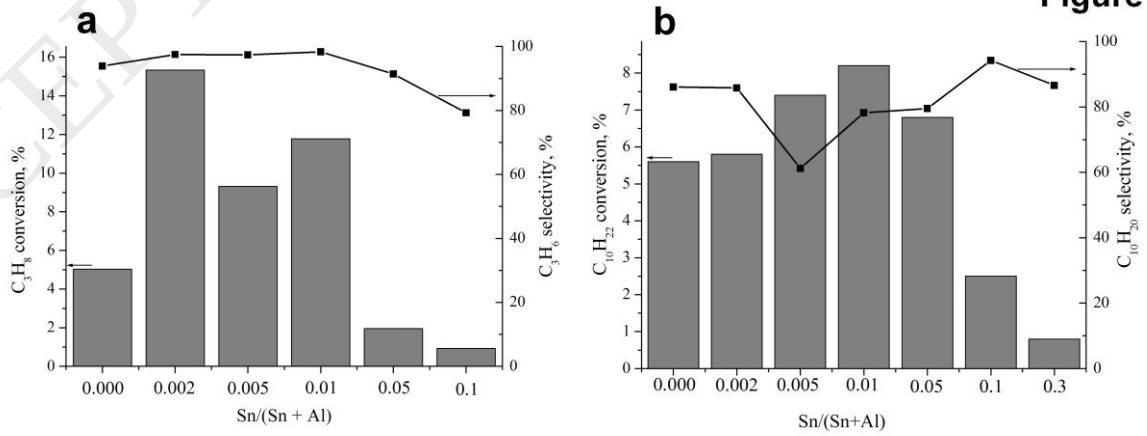

Table captions

Table 1. Chemical composition and calculated structural parameters of MgAl(Sn)-LDH samples with differents tin fractions. Before measuring the concentration, the samples were calcined at 823 K.

Table 2. Basic textural characteristics of the studied samples according to nitrogen adsorption data. The samples were calcined at 823 K.

Table 3. Parameters of samples microstructure obtained by simulation from experimental Sn*K* EXAFS spectra for 1%Pt/MgAl(Sn)O_x. (Sn/(Sn+Al) = 0, 0.1, 0.3, 0.7)

Table 4. Results of XPS study of 1%Pt/MgAl(Sn)O_x catalysts. Sn/(Sn+Al) = 0, 0.1, 0.3, 0.7.

Table 5. Parameters of samples microstructure obtained by simulation from experimental PtL_3 EXAFS spectra for 1%Pt/MgAl(Sn)O_x. (Sn/(Sn+Al) = 0, 0.1, 0.3, 0.7) .

Table 1.

Sample	Data of chemical analysis, wt.%			Atomic ratio Mg:Al:Sn	Mg/ (Al+Sn)	c, nm	a, nm*
	Mg	Al	Sn				
MgAl(Sn0)-CO_3	41.0	14.9	0	3:1:0	3.0	2.352	0.3066
MgAl(Sn0.002)- CO_3	42.4	15.7	0.14	3:0.99:0.001	3.0	-	-
MgAl(Sn0.005)- CO_3	42.3	15.6	0.34	3:1:0.005	3.0	-	-
MgAl(Sn0.01)- CO_3	40.0	13.8	0.68	3:0.9:0.01	3.2	-	-
MgAl(Sn0.05)- CO_3	36.6	11.0	2.6	3:0.8:0.04	3.5	2.348	0.3070
MgAl(Sn0.1)- CO_3	40.0	13.4	5.3	3:0.9:0.1:	3.0	2.342	0.3074
MgAl(Sn0.3)- CO_3	32.9	7.9	14.9	3:0.6:0.3	3.3	2.334	0.3088
MgAl(Sn0.7)- CO_3	28.7	2.8	31.2	3:0.3:0.7	3.2	2.336	0.3122
MgAl(Sn1.0)- CO_3	27.3	0	38.9	3:0:1.0	3.0	2.316	0.3143

* *a*, *c* (nm) – LHD lattice parameters

Table 2.

Sample	$S_{BET.}$, m^2 g^{-1}	$V_{ads,}$ sm^3 g^{-1}	D, nm
$MgAlO_x$	230	0.747	12.99
MgAl(Sn0.1)O_x	230	0.606	10.53
MgAl(Sn0.3)O_x	173	0.322	7.47
MgAl(Sn0.7)O_x	146	0.285	7.80
$MgSnO_x$	127	0.598	18.82

Table 3.

	1%Pt/MgAl(Sn-0.1)O_x		1%Pt/MgAl(Sn-0.3)O_x		1%Pt/MgAl(Sn-0.7)O_x	
	R Å	N	R, Å	N	R, Å	N
Sn-O	2.05	6.0	2.05	3.8	2.05	2.2
Sn-Pt			2.84	2.4	2.84	1.0
Sn-Sn			3.04	3.2	3.03	4.1
$(2\sigma^2)$ – O	0.010		0.011		0.014	
$(2\sigma^2)$ – Mg, Pt, Sn	0.025		0.026		0.024	
S_0^2			0.97			
Ef	-3.3		-5.9		-5.0	
fit	0.9		0.9		2.0	

Table 4.

Sample	Pt $3d_{5/2}$ binding energy (eV)	Pt/Mg	Sn $3d_{5/2}$ binding energy (eV)		Sn/SnO
			Sn	SnO	
1%Pt/MgAlO_x	2122.4	-	-	-	-
1%Pt/MgAl(Sn-0.1)O_x	2122.2	0.009	-	486.9	-
1%Pt/MgAl(Sn-0.3)O_x	2122.3	0.031	485.0	486.9	1.0
1%Pt/MgAl(Sn-0.7)O_x	2122.0	0.047	485.5	486.9	1.2
Pt^o (black)	2121.8				
Pt^{2+}	2123.5				

Table 5.

	1%Pt/MgAl(Sn-0.1)O_x		1%Pt/MgAl(Sn-0.3)O_x		1%Pt/MgAl(Sn-0.7)O_x	
	R Å	N	R, Å	N	R, Å	N
Pt – O	1.97	0.8	1.94	0.5	1.97	0.8
Pt – Cl	2.25	0.6	2.24	0.8	2.19	1.3
Pt – Pt	2.74	3.0	2.81	2.3	2.71	1.1
Pt – Sn	3.03	0.5	3.11	1.1	3.03	4.1
$(2\sigma^2)$ – O,Cl	0.008		0.009		0.011	
$(2\sigma^2)$ – Pt, Sn	0.018		0.027		0.021	
S_0^2			0.82			
Ef	-6.8		-5.9		-3.2	
fit	2.8		1.9		2.5	

N – partial coordination numbers, R - interatomic distances, Å, $2\sigma^2$ - Debye Waller factors, Fit - an index characterizing the quality of fitting. EXAFS spectra and parameters taken from the Structure Database [62]